

Characterization of kaolinite-cetyltrimethylammonium chloride intercalation complex synthesized through eco-friendly kaolinite-urea pre-intercalation complex

Éva Makó ^{a*}, András Kovács ^b, Richard Katona ^c, Tamás Kristóf ^d

^a Institute of Materials Engineering, University of Pannonia, H-8201 Veszprém, P.O. Box 158, Hungary, makoe@almos.vein.hu

^b Institute of Materials Engineering, University of Pannonia, H-8201 Veszprém, P.O. Box 158, Hungary, andree0717@gmail.com

^c Institute of Chemistry, Department of Physical Chemistry, University of Pannonia, H-8201 Veszprém, P.O. Box 158, Hungary, ricsidome@gmail.com

^d Institute of Chemistry, Department of Physical Chemistry, University of Pannonia, H-8201 Veszprém, P.O. Box 158, Hungary, kristoft@almos.vein.hu

*Corresponding author

Phone: 36-88-624-000/6065

E-mail address: makoe@almos.vein.hu (É. Makó)

ABSTRACT

Because of its suitability for producing kaolinite nanoscrolls, the kaolinite-cetyltrimethylammonium chloride intercalation complex is of interest in the research area of kaolinite nanocomposites. Experimental and molecular simulation analyses are used to investigate this intercalation complex, revealing its real structure formed through partially methoxy-modified kaolinite. Cost-efficient homogenization method is applied to synthesize the eco-friendly kaolinite-urea pre-intercalation complex, which was found to be favorable to intercalate cetyltrimethylammonium chloride into the interlayer space of kaolinite. The influence of the pre-intercalated urea molecules, the partial modification of kaolinite structure with methoxy groups, and the presence of methanol molecules in the interlayer space of kaolinite on the intercalation of cetyltrimethylammonium chloride is characterized experimentally by X-ray diffraction, thermal analysis, Fourier transform infrared spectroscopy, and electron microscopy. The kaolinite-cetyltrimethylammonium chloride complex is identified at the basal spacing of 3.82 nm with the chemical formula of $\text{Al}_2\text{Si}_2\text{O}_5(\text{OH})_{3.7}(\text{OCH}_3)_{0.3}(\text{CTAC})_{1.6}(\text{Me})_{1.6}$. Our molecular simulations predict methanol-containing structures between methoxy-functionalized kaolinite layers with diffuse guest molecular arrangements.

KEYWORDS

Kaolinite, Intercalation, Homogenization, Urea, Cetyltrimethylammonium chloride, Molecular simulation

1. INTRODUCTION

Various organic compounds (e.g. dimethyl sulfoxide, urea, N-methylformamide) can directly be intercalated into the interlayer space of kaolinite breaking up the hydrogen bonds between the double layers [1-41]. Kaolinite-dimethyl sulfoxide (kaolinite-DMSO), kaolinite-urea (kaolinite-U), and kaolinite-N-methylformamide (kaolinite-NMF) pre-intercalation complexes are successfully applied to synthesize advanced exfoliated kaolinite nanocomposites [18, 19, 25, 29-31, 34, 35, 40]. The preparation of these nanocomposites is usually carried out through multiple intercalations, where the natural platy kaolinite could transform from nanoplates into halloysite-like nanoscrolls. A promising exfoliation method for synthesizing kaolinite nanoscrolls involves the intercalation of cetyltrimethylammonium chloride (CTAC) into a kaolinite-methanol (kaolinite-Me) complex prepared from kaolinite-DMSO or kaolinite-NMF pre-intercalate [19, 29, 30, 34, 35, 40].

The frequently used precursors of the kaolinite-CTAC/kaolinite-Me complex (DMSO and NMF) are toxic and their industrial applications should be minimized [7, 19, 20, 29, 30, 33-36, 38, 40], while U is a non-toxic reagent and can intercalate into kaolinite in one step. To our knowledge, the preparation of kaolinite-CTAC complex using U as precursor was not published before. Direct intercalation of U into kaolinite was carried out using solution [1, 2, 4, 8, 9, 16, 20, 26, 28, 34, 37, 38], mechanochemical (co-grinding) [13, 21-23, 25-28, 31, 32, 37], and homogenization [41] techniques. These techniques resulted in high degree of intercalation, but the mechanochemical and homogenization techniques require less time and consume an order of magnitude less chemicals. According to our recent studies, higher degree of intercalation was obtained by the homogenization method than by the solution one, and the homogenization treatment (contrary to the mechanochemical one) does not reduce the amount of the crystalline kaolinite phase and does not crack the kaolinite layers, which may cause

difficulties in the formation of kaolinite nanoscrolls. Lately, we [41] applied the one-step homogenization technique to intercalate U.

Various researches [7, 10, 12, 15, 19, 20, 29, 30, 33-36, 38, 41] proved that kaolinite-DMSO and kaolinite-NMF complexes are effective pre-intercalates to form kaolinite-Me complexes. From the DMSO and NMF pre-intercalates, the formation of a kaolinite-Me complex with basal spacing of 1.11-1.13 nm was established in methanol-wet state [10, 12, 15, 19, 29, 30, 33-36, 41], but on air-drying, a contraction down to 0.93-0.86 nm was observed [12, 15, 19, 38, 41]. Using elemental and thermal analysis results, Tunney and Detellier [7], Komori et al. [15], and Matusik and Klapyta [36] calculated the values of $x=0.87$, $x=0.36$, and $x=0.48$, respectively, for the supposed chemical formula of $\text{Al}_2\text{Si}_2\text{O}_5(\text{OH})_{4-x}(\text{OCH}_3)_x$ for the obtained methoxylated kaolinite structure.

In spite of the more eco-friendly behavior of U, there are only two studies reported in the literature [34, 41], where the kaolinite-U pre-intercalate was used to synthesize kaolinite-Me complexes. In our previous work with U [41], we obtained the same methanol-wet state (with the basal spacing of 1.12 nm) as prepared earlier in the literature using the kaolinite-DMSO and kaolinite-NMF pre-intercalates [10, 12, 15, 19, 29, 30, 33-36]. However, the drying of our methanol-wet complex led to a somewhat different methoxylated kaolinite structure with $x=0.3$, which was far below the theoretical upper limit ratio of methoxy functionalization ($x=1$) of the inner surfaces.

Molecular simulation is a valuable tool to get a more complete understanding of experimental results. To our knowledge, there are no classical molecular simulation studies for kaolinite-CTAC complexes. Using atomically detailed molecular dynamics (MD) simulations, Zeng et al. [42] studied comparable systems with sufficiently large number of intercalated alkyl chains, but with a different clay mineral (montmorillonite). Recently, Zhang et al. [43] managed to employ such methodology for the kaolinite-dodecylamine system and

found the structure to be much more complicated than the idealized structure that can be obtained from stereochemical predictions.

In our previous study [41], we presented a detailed experimental and molecular simulation characterization of the possible wet and dry kaolinite-Me complexes. As a continuation of this research, in this work we synthesized, through the wet kaolinite-Me intermediate complex, the kaolinite-CTAC intercalation complex, which was further used to get kaolinite nanoscrolls. The experimental and theoretical characterizations of this complex consider the possibility of partial methoxy-functionalization of kaolinite layers and of the presence of free Me molecules in the interlayer space.

2. MATERIALS AND METHODS

2.1. Samples and intercalation procedure

The high-grade Zettlitz kaolin (ZK) [26, 41] was used, which contains 91 wt% of kaolinite with a Hinckley index (HI) [44] of around 0.8. Analytical grade urea (U), methanol (Me), and cetyltrimethylammonium chloride (CTAC) were used as intercalating reagent from Sigma-Aldrich, Scharlab, and Alfa Aesar, respectively.

The kaolinite-U and the kaolinite-Me complexes were prepared according to our previous work [41]. We synthesized the kaolinite-U pre-intercalation complex using our homogenization intercalation procedure: simply wetting kaolin with a mixture of solid U and distilled water in an agate mortar, and aging the mixture for 19 days in closed sample holder (the aged mixture is denoted as ZK-U). The kaolinite-Me complex was made by adding the pre-intercalation sample into Me and stirring the suspension for 24 h at room temperature [41]. After that, the solid part of the sample was separated and redispersed in a fresh portion

of Me, and this step was repeated 18 times. Then the centrifuged product was stored under Me for further use (the obtained kaolinite-Me complex sample is denoted as ZK-U-Me(wet)). A part of this type of sample was dried at room temperature for 24 h (it is denoted as ZK-U-Me(air-dry)).

The kaolinite-CTAC complex was prepared according to Yuan et al. [35]. 1.0 g of ZK-U-Me(wet) sample was added into 40 cm³ of Me based solution of CTAC (1 M) and stirred at 80 °C for 24 h. Then the solid part was separated by centrifugation. One portion of the solid was dried (it is denoted as ZK-U-Me-CTAC(unwashed)) and the other portion was washed 6 times with fresh ethanol, to remove CTAC, and then dried at 80 °C for 24 h (the obtained sample is denoted as ZK-U-Me-CTAC(washed)).

2.2. X-ray diffraction (XRD) analysis

The XRD patterns were recorded using a Philips PW 3710 type powder diffractometer with CuK α radiation, operating at 50 kV and 40 mA, a graphite diffracted-beam monochromator, and a continuous scanning speed of 0.02°/s. Data collections and evaluations were carried out with X'Pert Data Collector and X'Pert High Score Plus software. Profile fitting option of this software was applied to determine the full width at half-maximum (FWHM) value and the integral intensity of an individual diffraction peak. According to Wiewiora and Brindley [45], the integrated peak intensities of (001) reflections was used to determine the degree of intercalation. During the XRD measurement, wet samples were covered with a polyethylene foil to avoid drying. The (002) reflection of muscovite identified by 00-058-2035 reference pattern was used for internal low-2theta calibration [46].

2.3. Thermal analysis

Thermogravimetric (TG) experiments were carried out on 100-mg portions of the samples. The TG curves were recorded in a temperature range of 25-1000 °C with Derivatograph Q 1500D-type equipment (Hungarian Optical Works, Budapest), at a heating rate of 10 °C/min, in static air atmosphere, and using high-grade corundum as a reference sample. The total carbon, nitrogen, and hydrogen content of samples were determined thermally by a Carlo Erba EA1108 CHNS Elemental Analyzer equipment.

2.4. Fourier transform infrared (FTIR) spectroscopic analysis

The FTIR spectra of the samples were recorded in a Bruker Vertex70 spectrometer with Platinum ATR optics, at a resolution of 2 cm⁻¹, and with a room temperature DTGS detector (512 spectra were co-added). The spectra were processed with the GRAMS/AI version 9.0 program (Thermo Fischer Scientific, USA).

2.5. Electron microscopic analysis

Scanning electron microscopic (SEM) analyses were performed using a scanning electron microscope (ESEM Philips XL31) in the secondary electron mode. An accelerating voltage of 25 kV was applied. The samples were coated with gold/palladium films to a thickness of 2-3 nm using BALZERS SCD020 type equipment.

Transmission electron microscopy (TEM) was performed using a Philips CM20 TEM operated at 200-kV accelerating voltage for obtaining bright-field images and selected-area electron diffraction (SAED) patterns. The investigated samples were suspended in ethanol. The suspended particles were deposited directly onto Cu TEM grids covered with a lacey Formvar+carbon film.

2.6. Computational details

Constant pressure and temperature molecular dynamics (NpT-MD) simulations were performed with the GROMACS [47, 48] program package. The temperature and pressure controls were realized by using the Nosé-Hoover [49] and Parrinello-Rahman [50, 51] schemes, respectively. The pressure coupling was semi-isotropic: isotropic in the x- and y-directions, but different in the z-direction, which is perpendicular to the kaolinite layers. The leap-frog integrator was used with the integral time step of 1 fs. The van der Waals interactions were truncated at 1.2 nm and the periodic electrostatic interactions were calculated by the particle mesh Ewald (PME) [52] algorithm with 1.2 nm cutoff.

The composition of the kaolinite unit cell with C1 space group symmetry is $\text{Al}_2\text{Si}_2\text{O}_5(\text{OH})_4$ and the lattice parameters are $a = 0.5154$ nm, $b = 0.8942$ nm, $c = 0.7391$ nm, $\alpha = 91.93^\circ$, $\beta = 105.05^\circ$, $\gamma = 89.80^\circ$ [53]. We constructed a simulation box that consisted of four clay layers built from 96 double unit cells that are arranged in a 6x4x4 composition resulting in 816 atoms (96 Al atoms, 96 Si atoms, 432 O atoms, and 192 H atoms) per kaolinite layers. The layers were stacked upon each other forming four interlayer regions (periodic boundary conditions were applied in all three spatial directions). The initial atomic positions were set according to the experimental crystal structure of kaolinite [53]. The effect of partial grafting of Me molecules on the kaolinite inner surfaces was represented by replacing every sixteenth surface hydroxyl group of the kaolinite layers by a methoxy group [41]; this resulted in the unit cell composition of $\text{Al}_2\text{Si}_2\text{O}_5(\text{OH})_{3.75}(\text{OCH}_3)_{0.25}$.

In our simulations, we employed the framework of a standard fully flexible all-atom force field, CHARMM [54] and a recently proposed thermodynamically consistent force field, INTERFACE [55]. The parameters for kaolinite were taken from the INTERFACE force field (v1.3), which operates as an extension of common harmonic force fields (such as CHARMM) for inorganic compounds. The CHARMM27 force field variant implemented in GROMACS

[56] was used for CTAC and Me. The structure and the atomic charges of the Me model were adapted from the “Topology for the Charmm General Force Field v. 2b7 for Small Molecule Drug Design”. For the methoxy groups on the kaolinite surface, the CHARMM parameters of Me were used for the non-bonded interactions of the CH₃ group (excepting the charge parameter of H, which was reduced by ~10% to maintain charge neutrality) and the O-C bond stretching, and the Al-O-H equilibrium bond angle parameter [57] was accepted for the Al-O-C angle [41]. In all models the van der Waals nonbonded interactions were treated with the standard 12-6 Lennard-Jones potential, using the Lorentz-Berthelot combination rule. Only the H-bond vibrations (which are generally beyond the classical limit in these conditions) were constrained with the LINCS algorithm [58].

Because of the relatively slow convergence of the simulations with the investigated large flexible molecules (CTAC), special attention had to be taken when generating starting configurations for the production runs. The accepted procedure generates four different, quasi-gaseous guest molecules arrangements in the four interlayer spaces and it contains ‘pre-equilibration’ simulation periods. Initially, the guest molecules were created with random positions and orientations within artificially enlarged (~ three times larger than the expected final) interlayer spaces of the kaolinite. Then, after a short energy minimization of the system, two ‘pre-equilibration’ periods (a 1 and a 10 ns long) using the more robust Berendsen thermostat and barostat [59, 60] were applied, one with 100 and one with 10 times the final compressibility (system’s softness) parameter in the z-direction. The total subsequent simulation time using the Nosé-Hoover and Parrinello-Rahman schemes was 30 ns, with 10 ns long final averaging period, and the time step for the outputted trajectory frames was 1 ps.

3. RESULTS AND DISCUSSION

3.1. XRD analysis

As in our previous work [41], the XRD pattern of Zettlitz kaolin (Fig. 1, ZK) displays the (001) reflection at 0.72 nm of the original kaolinite and the (002) reflection of muscovite (M). In agreement with earlier reports [1, 2, 4, 8, 9, 13, 16, 20-23, 25-28, 34, 37, 38, 41], the intercalation of U into the interlayer space of kaolinite expands the 0.72-nm basal spacing, resulting in appearance of a new peak at 1.07 nm (ZK-U). In the XRD pattern of ZK-U-Me(wet), the complete displacement of U with Me and the formation of wet kaolinite-Me complex is clearly demonstrated by the shift of the whole (001) reflection from 1.07 nm to 1.11 nm [41]. The 1.11-nm basal spacing of the wet kaolinite-Me intercalation complex synthesized using the kaolinite-U pre-intercalation complex agrees well with the literature results with kaolinite-DMSO and kaolinite-NMF pre-intercalates [10, 12, 15, 19, 29, 30, 33-36, 41]. After drying the wet kaolinite-Me complexes at room temperature, the (001) reflections of the expanded phase decreased to 0.86 nm (ZK-U-Me(air-dry) sample), which is close to the value ($d_{001} = 0.88$ nm) reported by Cheng et al. [38] for similar air-dried complex prepared from kaolinite-U pre-intercalate. According to the literature [7, 15, 35, 41], the formation of the 0.86-nm complex from the 1.11-nm one can be attributed to the partial release of mobile Me and/or water molecules from the interlayer spaces during the air-drying process. After treating the wet kaolinite-Me intercalation complex with CTAC, the (001), (002), (003), (004), and (005) reflections of the kaolinite-CTAC intercalation complex [30, 35, 40] appeared at 3.82, 1.91, 1.27, 0.95, and 0.76 nm, respectively (ZK-U-Me-CTAC(unwashed) sample). The presence of these characteristic reflections, together with the disappearance of the 1.11-nm basal spacing, proves the complete formation of kaolinite-CTAC intercalation complex. Also, these intense reflections indicate that the intercalated

CTAC molecules enter into the interlayer spaces without separating the individual kaolinite layers. (Note that reflections related to CTAC crystals [30] adsorbed on the particle surfaces are also detected.) The XRD pattern of ZK-U-Me-CTAC(washed) shows the total disappearance of the reflections of kaolinite-CTAC intercalation complex, which means that CTAC molecules were removed from the interlayer space through washing with ethanol [30, 35, 40]. In agreement with previous observations [30, 35, 40], a small broad reflection at 0.88 nm can be identified here, indicating the presence of dry methoxy-modified kaolinite. As the 0.88-nm peak is more significantly broadened in the case of ZK-U-Me-CTAC(washed) than the 0.86-nm peak in the case of ZK-U-Me(air-dry), possibly the crystallite size along c axis (the thickness of kaolinite particles) of the expanded phase becomes smaller during the washing process (less ordering along c axis for the expanded phase seems improbable) [40].

The degrees of intercalation are 79%, 78%, 77% and 79% for ZK-U, ZK-U-Me(wet), ZK-U-Me(air-dry), and ZK-U-Me-CTAC(unwashed), respectively; these values confirm that the degree of intercalation with U determines the degree of further intercalation with Me and CTAC. Certainly, this also means that the mass fraction of non-intercalated phase is almost the same (~20%) for ZK-U, ZK-U-Me(wet), ZK-U-Me(air-dry), and ZK-U-Me-CTAC(unwashed). Using the integrated peak intensities of the 0.72-nm reflection of the unreacted kaolinite as reference both before and after the exfoliation step, we can get an estimated numerical value for the degree of exfoliation. Assuming that the calculated integrated peak intensities of the 0.72-nm reflection are nearly the same for ZK-U-Me-CTAC(unwashed) and ZK-U-Me-CTAC(washed), the degree of intercalation can be calculated as 38% for the 0.88-nm complex, and thus $79\% - 38\% = 41\%$ of the kaolinite-CTAC intercalation complex was transformed to kaolinite nanoscrolls (exfoliated kaolinite) during washing with ethanol. (To our knowledge, such estimation has not been used yet in the literature for the degree of exfoliation.)

3.2. Thermal analysis

The thermal stability and the chemical composition of the kaolinite-CTAC complex were studied before and after washing with ethanol (Fig. 2 and Table 1). The differential thermogravimetric (DTG) curve of the untreated kaolin (Fig. 2, ZK) shows two mass losses at 59 °C and 560 °C, which are related to the loss of the adsorbed water and the dehydroxylation of kaolinite, respectively [26, 41]. Heating the dried methanol-treated kaolin (ZK-U-Me(air-dry)), two mass losses were observed again. The first one (between 25 and 360 °C) is also due to the loss of the adsorbed water and Me, while the second one (between 360 and 1000 °C) can be attributed to the decomposition of methoxy groups together with dehydroxylation of kaolinite [7, 15, 41]. Similarly to previous reports, there is a small decrease in the dehydroxylation peak temperature (as compared to that of the untreated kaolin), which indicates the modification of the kaolinite structure with methoxy groups.

In the DTG curve of the sample treated with CTAC solution (Fig. 2, ZK-U-Me-CTAC(unwashed)), three major mass loss steps were observed. In the first step up to 165 °C, the adsorbed water and Me were removed. Similarly to previous investigations [61, 62], the oxidation of CTAC followed by the escape of volatile fragments and the formation of some kind of quasi-charcoal took place between 165 and 360 °C. Finally, the methoxy-modified kaolinite dehydroxylated, as well as the methoxy groups and quasi-charcoal completely decomposed between 360 and 1000 °C. The temperature of its DTG peak is by ~50 °C lower as compared to that of the dried methanol-treated kaolin. The DTG curve of pure CTAC (not presented) shows that its decomposition steps are very similar to that of the adsorbed and the intercalated CTAC. Between 165 and 360 °C, the pure CTAC and the ZK-U-Me-CTAC(unwashed) samples have a main mass loss of 89% and 55%, respectively. From this we can give the CTAC content of the ZK-U-Me-CTAC(unwashed) sample as ~60 wt% and, on the basis of our XRD measurements, it must be mainly intercalated CTAC. The DTG

curve of ZK-U-Me-CTAC(washed) is similar to that of ZK-U-Me(air-dry), which indicates that the CTAC molecules were practically removed from the interlayer space through washing with ethanol. At the same time, the mass loss step of ZK-U-Me-CTAC(washed) between 360 and 1000 °C shifted to lower temperature, and this reveals that the hydroxyl and methoxy groups became more weakly bonded after exfoliation.

Accepting our previously obtained value of $x=0.3$ for this methoxylated kaolinite structure with the chemical formula of $Al_2Si_2O_5(OH)_{4-x}(OCH_3)_x$ [41], the chemical composition of the kaolinite-CTAC complex can be calculated from the measured total carbon, nitrogen, and hydrogen content of the ZK-U-Me-CTAC(unwashed) and ZK-U-Me-CTAC(washed) samples (Table 1). Our estimation provided the formula of the kaolinite-CTAC complex as $Al_2Si_2O_5(OH)_{3.7}(OCH_3)_{0.3}(CTAC)_{1.6}(Me)_{1.6}$, which means that the interlayer molecular ratio of Me to CTAC is approximately 1:1. Using the molecular weights, the intercalated CTAC and mobile Me content of the ZK-U-Me-CTAC(unwashed) sample can be given as ~60 wt% and ~6 wt%, respectively. The data in Table 1 also prove that the washing with ethanol almost fully removed the CTAC molecules (the nitrogen content reduced by one order of magnitude) and, in view of the fact that the characteristic reflections of the kaolinite-CTAC intercalation complex are missing in the corresponding XRD pattern, the residual part (~6 wt%) seems to be adsorbed on the outer particle surfaces.

Table 1. Average carbon, hydrogen, and nitrogen content of kaolinite-CTAC complexes obtained from CHNS elemental analysis.

Sample	Carbon (wt%)	Hydrogen (wt%)	Nitrogen (wt%)
ZK-U-Me-CTAC(unwashed)	44.4	9.4	2.7
ZK-U-Me-CTAC(washed)	5.0	2.3	0.28

3.3. FTIR spectroscopic analysis

The FTIR spectra of the untreated and treated kaolins are shown in Fig. 3. In the spectrum of the untreated kaolin (ZK), the vibration bands at 3694, 3670, and 3654 cm^{-1} belong to the inner surface hydroxyl groups and the fourth band at 3620 cm^{-1} belongs to the inner hydroxyl group [22, 26, 28, 38, 63]. The major difference between the FTIR spectra of ZK and ZK-U is the appearance of the bands at 3498, 3410 and 3387 cm^{-1} and the weakening of the 3694 cm^{-1} band (as compared to the 3620 cm^{-1} band) in the case of ZK-U, which indicate hydrogen bonding between urea molecules and the tetrahedral sheets of kaolinite. These stretching vibrations of kaolinite-U complexes have been discussed in previous studies [26, 28, 38]. In the FTIR spectra of the dried methanol-treated kaolin (ZK-U-Me(air-dry)), these typical vibrations of kaolinite-U complexes practically disappeared and new bands at 3535 and 2842 cm^{-1} were detected, which reflects, in agreement with the findings of the XRD measurements, the complete substitution of U by Me species and the formation of methoxy-modified kaolinite structure (with possible mobile Me and/or water molecules) [35, 38]. After CTAC intercalation (ZK-U-Me-CTAC(unwashed)), some characteristic bands of the kaolinite-CTAC intercalation complex and CTAC molecules were observed at 3433, 3386, 3240, 3013, 2949, 2914, 2870, and 2849 cm^{-1} [38, 64]. The two most intense bands at 2914 and 2849 cm^{-1} can be assigned to the CH_2 asymmetric and symmetric stretching vibrations. All typical vibrations of the kaolinite-CTAC intercalation complex significantly decreased or vanished in the spectrum of ZK-U-Me-CTAC(washed), which also indicates, in accordance with the results of the XRD and thermal analyses, that the ethanol washing step completely removes the CTAC molecules from the interlayer space. The spectrum of the 3000-3800 cm^{-1} region of ZK-U-Me-CTAC(washed) resembles that of ZK-U-Me(air-dry), and the band at 3540 cm^{-1} is due to the existence of characteristic hydrogen bonding between kaolinite and Me.

3.4. Electron microscopic analysis

To characterize the morphology of the untreated and treated kaolins, SEM and TEM images were made. As indicated by the SEM image of the Zettlitz kaolin (Fig. 4A), the primary plate-like kaolinite particles have a diameter of between 0.5 μm and 5 μm , which can form loose aggregates and kaolinite books [22, 26]. The intercalation of U and Me did not modify the platy morphology of kaolinite (related images are not shown) [22, 26, 35, 40]. After CTAC intercalation, a slight curling of the edges of kaolinite plates was observed (B), which was caused by the large expansion of basal spacing up to 3.82 nm [30, 35, 40].

In the SEM (C) and TEM (D) images of the ZK-U-Me-CTAC(washed) sample the formation of kaolinite nanoscrolls is clearly shown; they have an average external diameter of ~ 25 nm with a wall thickness up to 6 nm. Their length ranges from 350 nm to 1250 nm, which seems to be mainly determined by the diameter of the original kaolinite plates. In harmony with our XRD results, the TEM image also demonstrates the coexistence of such completely exfoliated phase (nanoscrolls) with incompletely exfoliated and non-intercalated phases (partially rolled and unaffected plates).

3.5. Molecular simulations

NpT-MD simulations were carried out at 298 K and 1.013 bar for different system's compositions to model conceivable intercalation complexes with kaolinite, CTAC and Me (the adsorption on the outer surface of the kaolinite particles was ruled out). The first series of NpT-MD simulations was performed with regular kaolinite and CTAC to identify possible regions of interest of interlayer loading. The calculated basal spacing showed a nearly linear relationship with the guest molecule content up to ~ 60 wt%, where the CTAC content of 58.7 wt% gave the nearest basal spacing (3.81 nm) to that obtained by our XRD measurements. The subsequent simulations revealed that the presence of grafted methoxy groups on the inner

kaolinite surfaces does not meaningfully affect the composition at these high guest-molecular proportions. We could reproduce our experimental basal spacing (3.82 nm) at the CTAC content of 58.4 wt%; the 0.3-wt% difference only reflects the slightly larger mass of the methoxy-modified kaolinite layers.

Based on the existing synthesis procedures, however, it is reasonable to assume (even in lack of other experimental information) that the real kaolinite-CTAC complex can contain mobile Me molecules. To investigate this possibility, we conducted a number of simulations with varying guest molecule contents, keeping the interlayer molecular ratios of Me to CTAC as 1:1, 2:1, 5:1 and 10:1. Table 2 indicates the compositions that resulted in basal spacing values around the experimentally detected one. At ratios of 5:1 and 10:1, two cases were considered, because here the experimental basal spacing could be reproduced with greater errors. From Table 2, one feature of the complexes is immediately visible: the total guest molecule content is always about 58-59 wt%, independently of the molecular ratios of the guest molecules, and this specifies a fairly constant 10% space requirement of a Me molecule in the interlayer space as compared to that of a CTAC molecule.

Table 2. Compositions and calculated basal spacings of the conceivable kaolinite-CTAC-Me intercalation complexes with the indicated molecular ratios of Me to CTAC, obtained from NpT-MD simulations at 298 K and 1.013 bar (r. stands for *regular* kaolinite; the other complexes contain methoxy-modified kaolinite; n denotes the number of guest molecules per kaolinite unit cell).

Me:CTAC	wt% _{CTAC}	n_{CTAC}	wt% _{Me}	n_{Me}	basal spacing (nm)
0:1 (r.)	58.7	1.146	-	-	3.81
0:1	58.4	1.146	-	-	3.82
1:1	53.0	1.042	5.3	1.042	3.81
2:1	49.1	0.979	9.8	1.958	3.82
5:1	39.5	0.792	19.8	3.958	3.84
5:1*	39.0	0.771	19.5	3.854	3.76
10:1	29.4	0.583	29.4	5.833	3.86
10:1*	28.9	0.563	29.0	5.625	3.74

For the conceivable complexes, the density distributions of the guest molecules (Fig. 5) along the axis perpendicular to the clay layers do not show well-layered structures. The location of the outside peaks of the cetyltrimethylammonium cations (CTA⁺) already suggests a parallel alignment of these chains with the clay layers (A) and the variation of these peak intensities indicates greater affinity to the tetrahedral sheets. In contrast, the chloride ions (B) have greater affinity to the octahedral sheets possessing slightly positive surface polarity. Undoubtedly, the chloride ions and the Me molecules (C) can get closer to the clay surfaces.

The $\cos\theta$ distributions of the guest molecules (Fig. 6) suggest a predominantly parallel ($\cos\theta=0$) alignment of CTA⁺ ions (A) with the kaolinite layers. A smaller proportion of CTA⁺ chains that are nearly in perpendicular alignment to the clay layers tend to point with their polar head (as a result of the asymmetry in the chloride distribution) towards the octahedral sheets. The Me molecules (B) exhibit a quite diffuse molecule arrangement but their dipole moment vectors point towards the tetrahedral sheet with greater probability. The curves for the end-to-end distance distribution of CTA⁺ chains (C) show that the chains roughly keep their linear shape between the clay layers and the average stiffness of these chains, related to the sharpness of the curves, is generally larger at higher methanol content.

Representative simulation snapshots in Fig. 7 illustrate the preference of the CTA⁺ chains to align in parallel to the kaolinite plates, though quite a few chains find favorable positions through utilizing their flexibility. Visual inspections of several additional simulation snapshots give some indication of demixing at molecular ratios higher than 2:1 (e.g. snapshot C) revealing alternating CTA⁺ clusters and island-like Me-rich regions; this fact is against the likelihood that Me-rich complexes can be synthesized in the experiments.

From the outputted trajectory frames of the simulations, we calculated the average minimum image intermolecular energies in such a way that only the guest molecule-guest molecule and guest molecule-kaolinite interactions within the same interlayer space were

summed (Fig. 8). This enabled us to approximate the cohesive energy between the kaolinite layers for the conceivable complexes at the investigated high guest molecule contents. The results seem to show that mobile Me molecules prefer to remain in or enter into the interlayer space but, at the same time, support the unlikeliness of the Me-rich composition range. The highest absolute cohesive energies were obtained at the molecular ratios of 1:1 and 2:1, which is in acceptable agreement with the conclusion of our elemental analysis.

4. CONCLUSIONS

We could successfully produce the kaolinite-CTAC intercalation complex through the kaolinite-U pre-intercalation and kaolinite-Me intermediate complexes, which seems to be a promising, simple, and non-toxic route for the potential industrial production of kaolinite nanoscrolls. Our XRD results showed that the CTAC molecules enter into the interlayer spaces without causing loss of periodicity in the stacking of kaolinite layers, and expand the basal spacing to 3.82 nm. The same high degree of intercalation (~80%) could be achieved for this complex as for the kaolinite-U and kaolinite-Me complex, which confirms that the intercalation with CTAC is determined by the first intercalation with U. In addition to the expected methoxy functionalization of kaolinite-Me complexes [30, 35, 40, 41], the undertaken XRD, thermal and FTIR analyses evidenced the continued existence of methoxy-functionalized inner kaolinite surfaces after the CTAC treatment. Furthermore, the prepared kaolinite-CTAC intercalation complex proved to be favorable to produce, by washing it with ethanol, kaolinite nanoscrolls (completely exfoliated phase), which are similar to those obtained through DMSO and NMF as precursors [30, 35, 40]. Our molecular simulations revealed the possible compositions of the 3.82-nm complex. Using the highly realistic

CHARMM/INTERFACE force field system, this modeling could completely take account of the interactions among the intercalated molecules, and predicted a methanol-containing structure with interlayer molecular ratio of 1:1 or 2:1. The formula of $\text{Al}_2\text{Si}_2\text{O}_5(\text{OH})_{3.7}(\text{OCH}_3)_{0.3}(\text{CTAC})_{1.6}(\text{Me})_{1.6}$, estimated from thermal analysis results, corresponds to the 1:1 molecular ratio of Me to CTAC. The simulated interlayer structure of CTAC deviates from the literature assumption obtained from stereochemical calculations (ideal tilted bilayer; see, e.g. the schematic representation in [35] and [40]): it does not show any distinct layering, and the most probable orientation of the chains is parallel to the kaolinite plates.

ACKNOWLEDGEMENT

We gratefully acknowledge the support of the Hungarian National Research Fund [OTKA NN113527] in the framework of ERA Chemistry.

REFERENCES

- [1] A. Weiss, Eine Schichteinschlußverbindung von Kaolinit mit Harnstoff, *Angew. Chem.* 73 (1961) 736-737.
- [2] A. Weiss, W. Thielepape, G. Göring, W. Ritter, H. Schaffer, Kaolinit-Einlagerungs-Verbindungen, in: T. Rosenquist, P. Graff-Pettersen (Eds.), *Proceedings of the International Clay Conference, Stockholm, 1963*, pp. 287-305.
- [3] S. Olejnik, L.A.G. Aylmore, A.M. Posner, J.P. Quirk, Infrared spectra of kaolin mineral-dimethyl sulfoxide complexes, *J. Phys. Chem.* 72 (1968) 241-249.
- [4] G. Lagaly, Clay-organic interaction, *Phil. Trans. R. Soc. London. A* 311 (1984) 315-332.
- [5] J.G. Thompson, C. Cuff, Crystal structure of kaolinite:dimethyl sulfoxide intercalate, *Clays Clay Miner* 33 (1985) 490-500.
- [6] G. J. Churchman, Relevance of different intercalation tests for distinguishing halloysite from kaolinite in soils, *Clays Clay Miner* 38 (1990) 591-599.
- [7] J.J. Tunney, C. Detellier, Chemically modified kaolinite. Grafting of methoxy groups on the interlamellar aluminol surface of kaolinite, *J. Mater. Chem.* 6 (1996) 1679-1685.
- [8] R.L. Frost, T.H. Tran, J. Kristóf, FT-Raman spectroscopy of the lattice region of kaolinite and its intercalates, *Vib. Spectrosc.* 13 (1997) 175-186.
- [9] J. Kristóf, R.L. Frost, E. Horváth, L. Kocsis, J. Inczedy, Thermoanalytical investigations on intercalated kaolinites, *J. Therm. Anal.* 53 (1998) 467-475.
- [10] Y. Komori, Y. Sugahara, K. Kuroda, A kaolinite-NMF-methanol intercalation compound as a versatile intermediate for further intercalation reaction of kaolinite, *J. Mater. Res.* 13 (1998) 930-934.

- [11] J. Kristóf, R.L. Frost, J.T. Klopprogge, E. Horváth, M. Gábor, Thermal behaviour of kaolinite intercalated with formamide, dimethyl sulphoxide and hydrazine, *J. Therm. Anal. Cal.* 56 (1999) 885-891.
- [12] Y. Komori, Y. Sugahara, K. Kuroda, Intercalation of alkylamines and water into kaolinite with methanol kaolinite as an intermediate, *Appl. Clay Sci.* 15 (1999) 241-252.
- [13] K. Tsunematsu, H. Tateyama, Delamination of urea–kaolinite complex by using intercalation procedures, *J. Am. Ceram. Soc.* 82 (1999) 1589–1591.
- [14] R.L. Frost, J. Kristóf, E. Horváth, J.T. Klopprogge, Deintercalation dimethyl sulphoxide intercalated kaolinites – a DTA/TGA and Raman spectroscopic study, *Thermochim. Acta* 327 (1999) 155-166.
- [15] Y. Komori, H. Enoto, R. Takenawa, S. Hayashi, Y. Sugahara, K. Kuroda, Modification of the interlayer surface of kaolinite with methoxy groups, *Langmuir* 16 (2000) 5506-5508.
- [16] R.L. Frost, J. Kristof, L. Rintoul, J.Th. Klopprogge, Raman spectroscopy of urea and urea-intercalated kaolinites at 77 K, *Spectrochim. Acta Part A* 56 (2000) 1681-1691.
- [17] J.E. Gardolinski, F. Wypych, M.P. Cantao, Exfoliation and hydration of kaolinite after intercalation with urea, *Quim. Nova* 24 (2001) 761-767.
- [18] J.E.F.C. Gardolinski, G. Lagaly, Grafted organic derivatives of kaolinite: II. Intercalation of primary n-alkylamines and delamination, *Clay Miner.* 40 (2005) 547-556.
- [19] J.E.F.C. Gardolinski, Interlayer grafting and delamination of kaolinite, PhD Thesis, Kiel, 2005.
- [20] F. Bergaya, B.K.G. Theng, G. Lagaly, *Handbook of Clay Science, Developments in Clay Science*, Vol. 1, Elsevier, 2006.
- [21] S. Letaief, T.A. Elbokl, C. Detellier, Reactivity of ionic liquids with kaolinite: Melt intercalation of ethyl pyridinium chloride in an urea-kaolinite pre-intercalate, *J. Colloid Interface Sci.* 302 (2006) 254-258.

- [22] M. Valaskova, M. Rieder, V. Matejka, P. Capkova, A. Sliva, Exfoliation/delamination of kaolinite by low-temperature washing of kaolinite-urea intercalates, *Appl. Clay Sci.* 35 (2007) 108-118.
- [23] C.R.B. Fukamachi, F. Wypych, A.S. Mangrich, Use of Fe^{3+} ion probe to study the stability of urea-intercalated kaolinite by electron paramagnetic resonance, *J. Colloid Interface Sci.* 313 (2007) 537-541.
- [24] S. Letaief, I.K. Tonle, T. Diaco, C. Detellier, Nanohybrid materials from interlayer functionalization of kaolinite. Application to the electrochemical preconcentration of cyanide, *Appl. Clay Sci.* 42 (2008) 95-101.
- [25] S. Letaief, C. Detellier, Clay-polymer nanocomposite material from the delamination of kaolinite in the presence of sodium polyacrylate, *Langmuir* 25 (2009) 10975-10979.
- [26] É. Makó, J. Kristóf, E. Horváth, V. Vágvölgy, Kaolinite–urea complexes obtained by mechanochemical and aqueous suspension techniques - A comparative study, *J. Colloid Interface Sci.* 330 (2009) 367-373.
- [27] G. Rutkai, É. Makó, T. Kristóf, Simulation and experimental study of intercalation of urea in kaolinite, *J. Colloid Interface Sci.* 334 (2009) 65-69.
- [28] E. Horváth, J. Kristóf, R.L. Frost, Vibrational Spectroscopy of Intercalated Kaolinites. Part I., *Appl. Spectrosc. Rev.* 45 (2010) 130-147.
- [29] J. Matusik, E. Wisła-Walsh, A. Gaweł, E. Bielanska, K. Bahranowski, Surface area and porosity of nanotubes obtained from kaolin minerals of different structural order, *Clays Clay Miner.* 59 (2011) 116-135.
- [30] Y. Kuroda, K. Ito, K. Itabashi, K. Kuroda, One-Step Exfoliation of Kaolinites and Their Transformation into Nanoscrolls, *Langmuir* 27 (2011) 2028-2035.

- [31] S. Letaief, J. Leclercq, Y. Liu, C. Detellier, Single Kaolinite Nanometer Layers Prepared by an In Situ Polymerization-Exfoliation Process in the Presence of Ionic Liquids, *Langmuir* 27 (2011) 15248-15254.
- [32] H. Cheng, Q. Liu, J. Yang, S. Ma, R.L. Frost, The thermal behavior of kaolinite intercalation complexes-A review, *Thermochim. Acta* 545 (2012) 1-13.
- [33] J. Matusik, E. Scholtzova, D. Tunega, Influence of synthesis conditions on the formation of a kaolinite-methanol complex and simulation of its vibrational spectra, *Clays Clay Miner.* 60 (2012) 227-239.
- [34] F. Bergaya, G. Lagaly, *Handbook of Clay Science, Developments in Clay Science, Vol. 5*, Elsevier, Amsterdam, 2013.
- [35] P. Yuan, D. Tan, F. Annabi-Bergaya, W. Yan, D. Liu, Z. Liu, From platy kaolinite to aluminosilicate nanoroll via one-step delamination of kaolinite: Effect of the temperature of intercalation, *Appl. Clay Sci.* 83-84 (2013) 68-76.
- [36] J. Matusik, Z. Kłapyta, Characterization of kaolinite intercalation compounds with benzylalkylammonium chlorides using XRD, TGA/DTA and CHNS elemental analysis, *Appl. Clay Sci.* 83-84 (2013) 433-440.
- [37] É. Makó, J. Kristóf, E. Horváth, V. Vágvölgyi, Mechanochemical intercalation of low reactivity kaolinite, *Appl. Clay Sci.* 83-84 (2013) 24-31.
- [38] H. Cheng, X. Hou, Q. Liu, X. Li, R.L. Frost, New insights into the molecular structure of kaolinite-methanol intercalation complexes, *Appl. Clay Sci.* 109-110 (2015) 55-63.
- [39] S. Zhang, Q. Liu, H. Cheng, F. Zeng, Combined experimental and theoretical investigation of interactions between kaolinite inner surface and intercalated dimethyl sulfoxide, *Appl. Surface Sci.* 331 (2015) 234-240.

- [40] Q. Liu, X. Li, H. Cheng, Insight into the self-adaptive deformation of kaolinite layers into nanoscrolls, *Appl. Clay Sci.* 124-125 (2016) 175-182.
- [41] É. Makó, A. Kovács, Z. Ható, T. Kristóf, Simulation assisted characterization of kaolinite–methanol intercalation complexes synthesized using cost-efficient homogenization method, *Appl. Surface Sci.* 357 (2015) 626–634.
- [42] Q.H. Zeng, A.B. Yu, G.Q. Lu, R.K. Standish, Molecular Dynamics Simulation of Organic-Inorganic Nanocomposites: Layering Behavior and Interlayer Structure of Organoclays, *Chem. Mater.* 15 (2003) 4732-4738.
- [43] S. Zhang, Q. Liu, H. Cheng, X. Li, F. Zeng, R.L. Frost, Intercalation of dodecylamine into kaolinite and its layering structure investigated by molecular dynamics simulation, *J. Colloid Interface Sci.* 430 (2014) 345–350.
- [44] D.N. Hinckley, Variability in “crystallinity” values among the kaolin deposits of the coastal plain of Georgia and South Carolina, *Clays Clay Miner.* 11 (1963) 229-235.
- [45] A. Wiewiora, G. W. Brindley, Potassium acetate intercalation in kaolinites and its removal: effect of material characteristics. In: Heller, L. (Ed.), *Proceedings of the International Clay Conference Tokyo*. Israel University Press, Jerusalem, 1969, pp. 723–733.
- [46] D.L. Bish, J.E. Post, *Modern Powder Diffraction*, The Mineralogical Society of America, Washington, DC, 1989.
- [47] H.J.C. Berendsen, D. van der Spoel, R. van Drunen, GROMACS: A message-passing parallel molecular dynamics implementation, *Comput. Phys. Commun.* 91 (1995) 43-56.
- [48] B. Hess, C. Kutzner, D. van der Spoel, E. Lindahl, GROMACS 4: Algorithms for highly efficient, load-balanced, and scalable molecular simulation, *J. Chem. Theory Comput.* 4 (2008) 435-447.
- [49] W. G. Hoover, Canonical dynamics: equilibrium phase-space distributions, *Phys. Rev. A* 31 (1985) 1695-1697.

- [50] M. Parrinello, A. Rahman, Polymorphic transitions in single crystals: A new molecular dynamics method, *J. Appl. Phys.* 52 (1981) 7182-7190.
- [51] S. Nose, M. L. Klein, Constant pressure molecular dynamics for molecular systems, *Mol. Phys.* 50 (1983) 1055-1076.
- [52] T. Darden, D. York, L. Pedersen, Particle mesh Ewald: An $N \log(N)$ method for Ewald sums in large systems, *J. Chem. Phys.* 98 (1993) 10089-10092.
- [53] D.L. Bish, Rietveld refinement of the kaolinite structure at 1.5 K, *Clays Clay Miner.* 41 (1993) 738-744.
- [54] A.D. MacKerell Jr., Atomistic Models and Force Fields. in: O.M. Becker, A.D. MacKerell Jr., B. Roux, M. Watanabe (eds) *Computational Biochemistry and Biophysics*, Marcel Dekker, Inc. New York, 2001, pp. 7-38.
- [55] H. Heinz, T.J. Lin, R.K. Mishra, F.S. Emami, Thermodynamically consistent force fields for the assembly of inorganic, organic, and biological nanostructures: The INTERFACE force field, *Langmuir* 29 (2013) 1754-1765.
- [56] P. Bjelkmar, P. Larsson, M.A. Cuendet, B. Bess, E. Lindahl, Implementation of the CHARMM force field in GROMACS: Analysis of protein stability effects from correction maps, virtual interaction sites, and water models, *J. Chem. Theory Comput.* 6 (2010) 459-466.
- [57] N. W. Mitzel, Ch. Lustig, A hydrogen bonded aluminium alkoxide hydroxide aggregate resulting from the exposure of methylaluminium dichloride to air, *Z. Naturforsch.* 58b (2003) 489-492.
- [58] B. Hess, P-LINCS: A parallel linear constraint solver for molecular simulation, *J. Chem. Theory Comput.* 4 (2008) 116-122.
- [59] G. Bussi, D. Donadio, M. Parrinello, Canonical sampling through velocity rescaling, *J. Chem. Phys.* 126 (2007) 014101-1-7.

- [60] H.J.C. Berendsen, J.P.M. Postma, A. DiNola, J.R. Haak, Molecular-dynamics with coupling to an external bath, *J. Chem. Phys.* 81 (1984) 3684-3690.
- [61] H. He, Z. Ding, J. Zhu, P. Yuan, Y. Xi, D. Yang, R.L. Frost, Thermal characterization of surfactant-modified montmorillonite, *Clays Clay Min.* 53 (2005) 287–293.
- [62] I. Lapidés, M. Borisover, S. Yariv, Thermal analysis of hexadecyltrimethylammonium-montmorillonites, *J. Therm. Anal. Cal.* 105 (2011) 921-929.
- [63] V.C. Farmer, *The Infrared Spectra of Minerals*, Mineralogical Society, London, 1974.
- [64] Z.H. Li, W.T. Jiang, H.L. Hong, An FTIR investigation of hexadecyltrimethylammonium intercalation into rectorite, *Spectrochim. Acta A Mol. Biomol. Spectrosc.* 71 (2008) 1525–1534.

FIGURE CAPTIONS

Fig. 1. XRD patterns of the Zettlitz kaolin (ZK), the ZK after treated with U (ZK-U), the ZK-U treated with Me in wet state (ZK-U-Me(wet)) and air-dried state (ZK-U-Me(air-dry)), the ZK-U-Me(wet) treated with CTAC (ZK-U-Me-CTAC(unwashed)), and the ZK-U-Me-CTAC(unwashed) washed with ethanol (ZK-U-Me-CTAC(washed)). (The degrees of intercalation, the FWHM values of the peaks of expanded and non-expanded kaolinite and their peak positions are indicated. M: muscovite; +: CTAC.)

Fig. 2. DTG curves of the Zettlitz kaolin (ZK), the ZK-U treated with Me in air-dried state (ZK-U-Me(air-dry)), the ZK-U-Me(wet) treated with CTAC (ZK-U-Me-CTAC(unwashed)), and the ZK-U-Me-CTAC(unwashed) washed with ethanol (ZK-U-Me-CTAC(washed)). (The DTG peak temperatures and the mass losses are indicated.)

Fig. 3. FTIR spectra of the Zettlitz kaolin (ZK), the ZK after treated with U (ZK-U), the ZK-U treated with Me in air-dried state (ZK-U-Me(air-dry)), the ZK-U-Me(wet) treated with CTAC (ZK-U-Me-CTAC(unwashed)), and the ZK-U-Me-CTAC(unwashed) washed with ethanol (ZK-U-Me-CTAC(washed)).

Fig. 4. SEM images of the Zettlitz kaolin (A), the ZK-U-Me-CTAC(unwashed) sample (B), and the ZK-U-Me-CTAC(washed) sample (C), as well as TEM image of the ZK-U-Me-CTAC(washed) sample (D).

Fig. 5. Density distributions of CTA^+ ions (A), Cl^- ions (B) and Me molecules (C) relative to the clay layers for the conceivable methoxy-modified kaolinite-CTAC-Me intercalation

complexes with the indicated molecular ratios of Me to CTAC. r is the distance from the center of mass of the lower kaolinite layer with octahedral upper sheet in the direction perpendicular to the clay layers. For visual reasons the distributions of CTAC at molecular ratio of 5:1 are not shown in this figure.

Fig. 6. $\cos\theta$ distributions of CTA^+ ions (A) and Me molecules (B), and the average relative end-to-end distance of CTA^+ chains (C) for the conceivable methoxy-modified kaolinite-CTAC-Me intercalation complexes with the indicated molecular ratios of Me to CTAC. θ is the angle between the normal vector of the kaolinite layers (pointing towards the tetrahedral surface of the neighboring layers) and the electro-inertial dipole moment vector of the CTA^+ ion or the methoxy group of Me. d_0 is the end-to-end distance of the straight CTA^+ chain. For visual reasons the $\cos\theta$ distribution of CTA^+ at molecular ratio of 5:1 is not shown in this figure.

Fig. 7. Simulation snapshots with methoxy-modified kaolinite at various molecular ratios of Me to CTAC ((A) - 0:1, (B) - 2:1, (C) - 10:1). The CPK color convention is used for the atoms except for carbon (cyan).

Fig. 8. Average total minimum image intermolecular energy of the (guest-guest + guest-kaolinite) interactions for the conceivable kaolinite-CTAC-Me intercalation complexes with the indicated molecular ratios of Me to CTAC, obtained from NpT-MD simulations at 298 K and 1.013 bar (r. stands for *regular* kaolinite; the other complexes contain methoxy-modified kaolinite).

Figure1

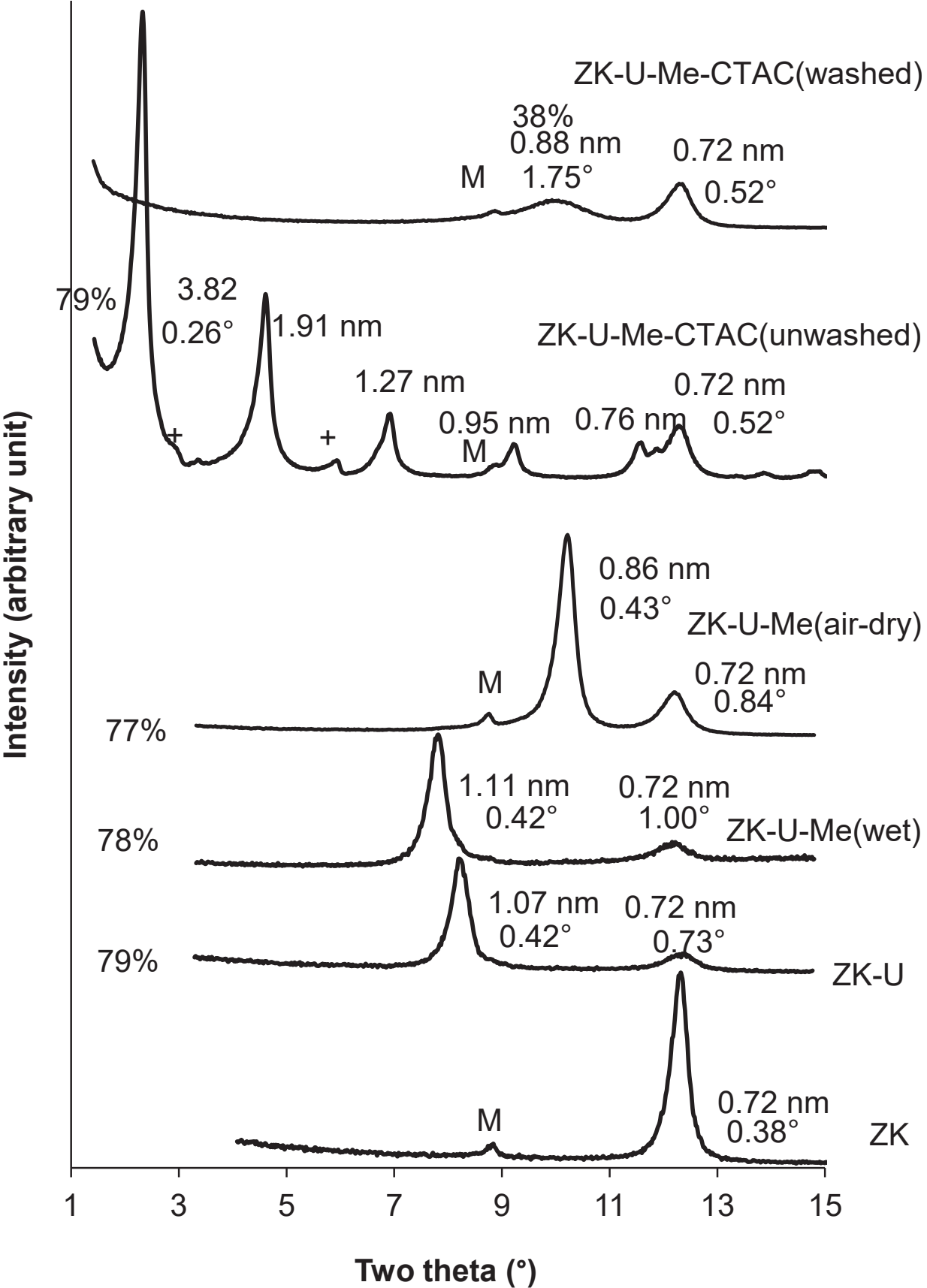


Figure2

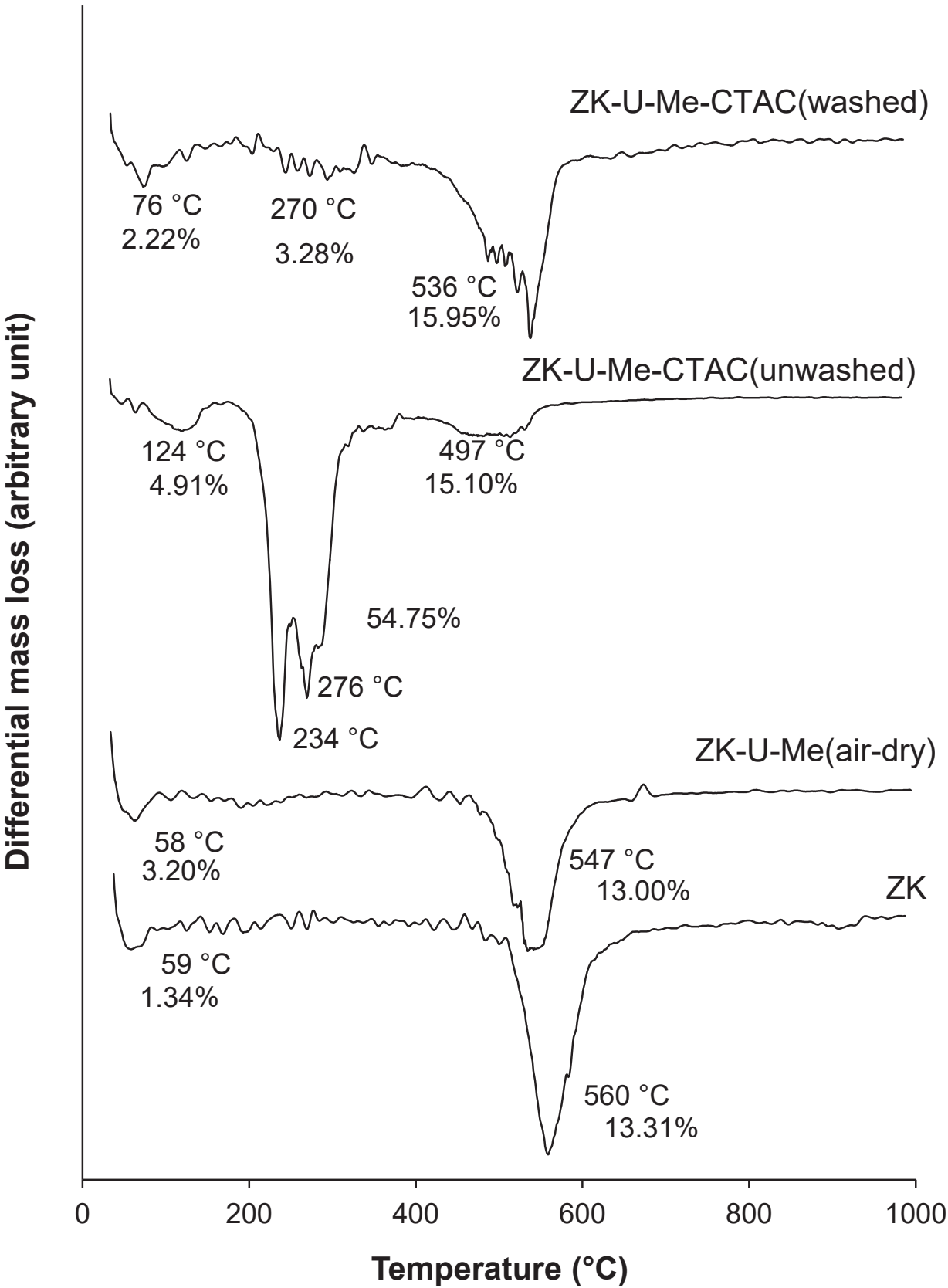


Figure3

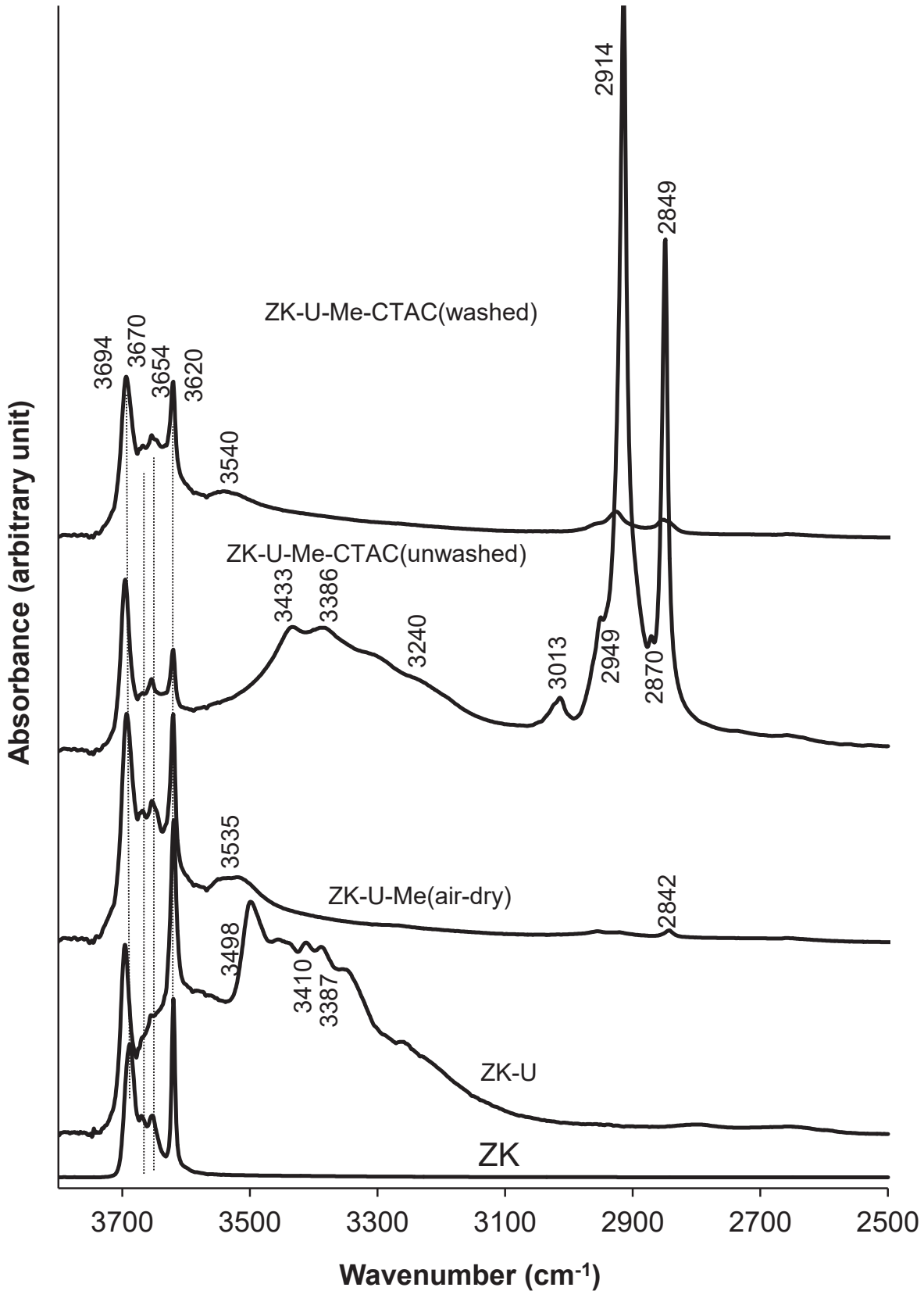


Figure4A
[Click here to download high resolution image](#)

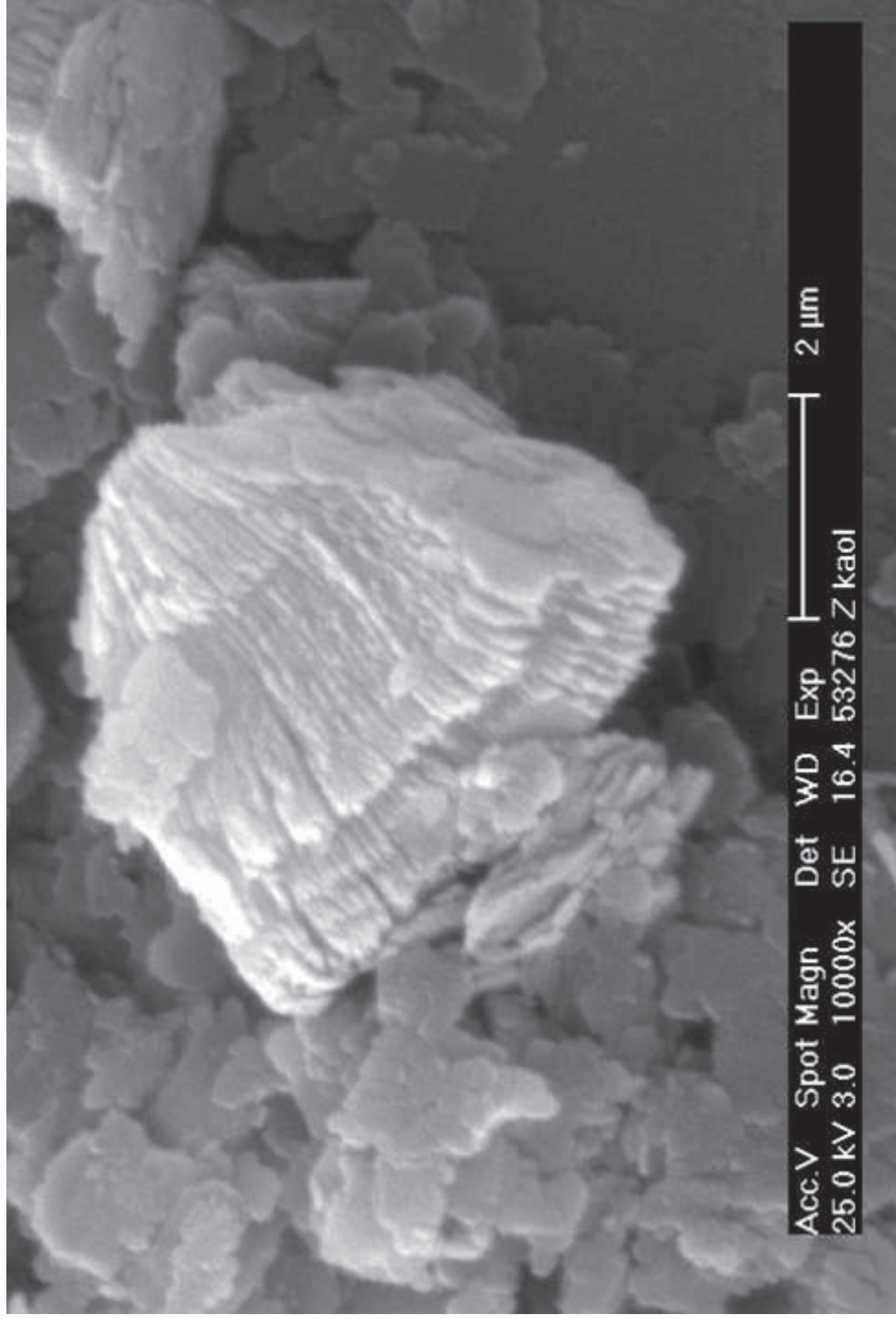


Figure4B
[Click here to download high resolution image](#)

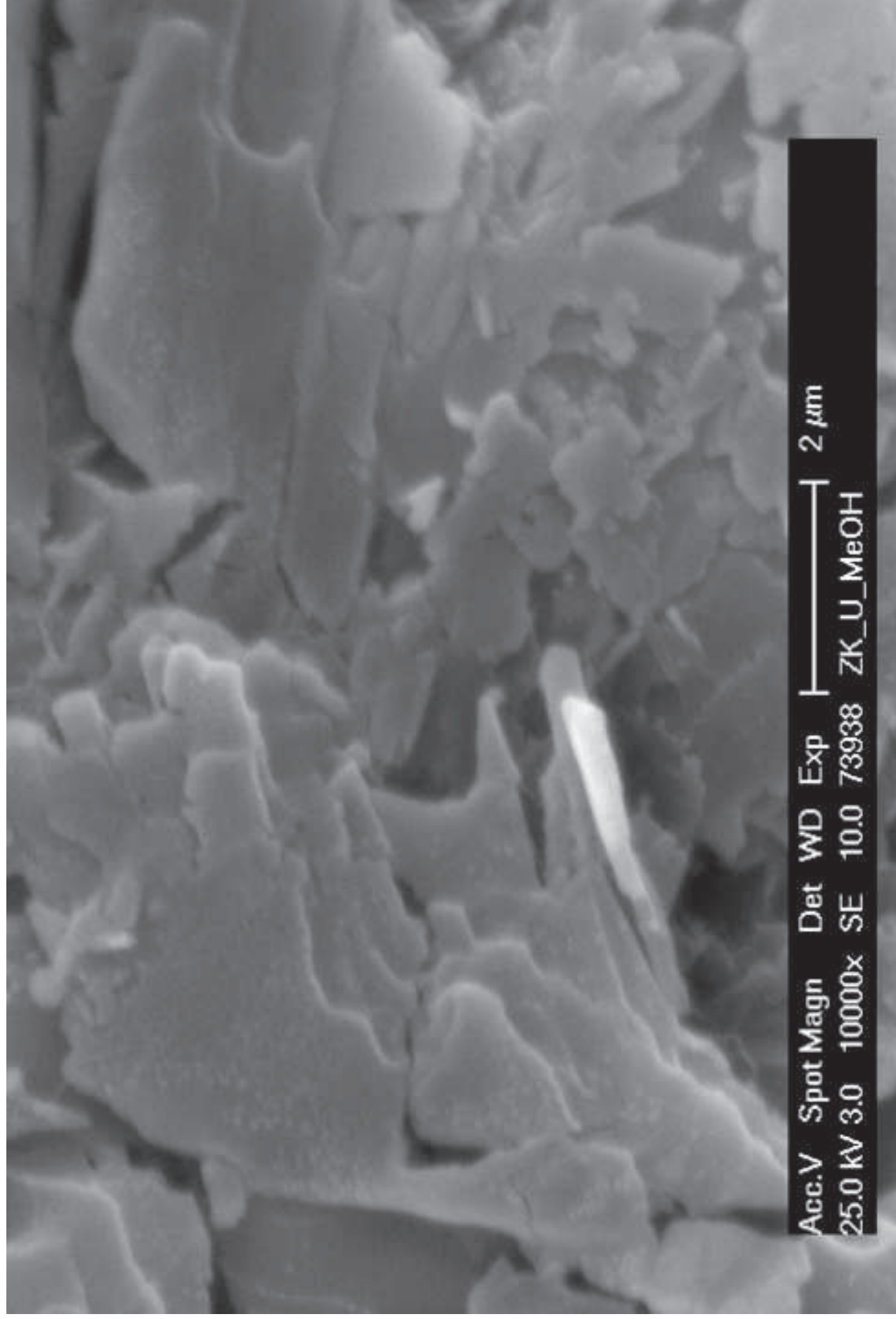


Figure4C
[Click here to download high resolution image](#)

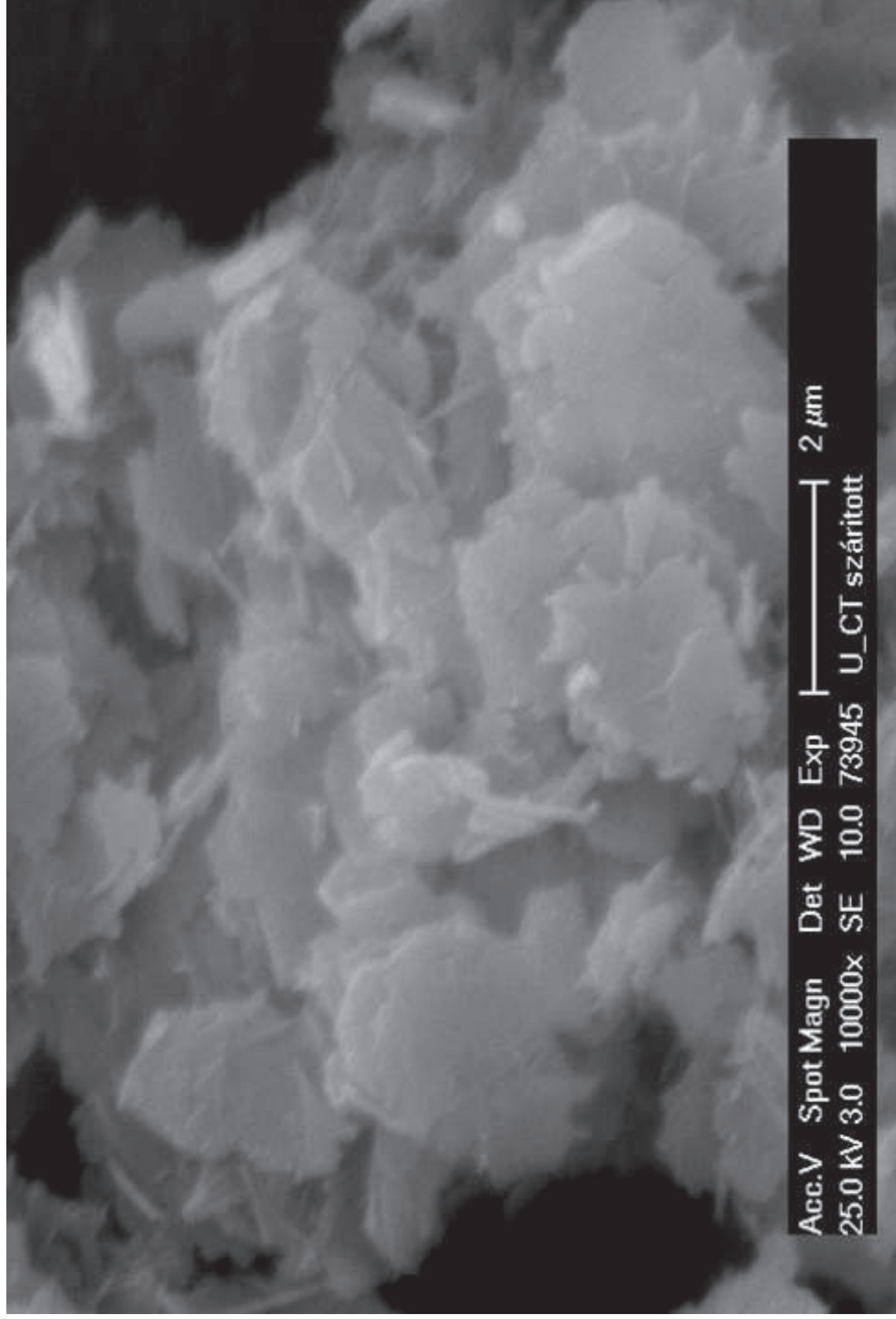


Figure4D
[Click here to download high resolution image](#)

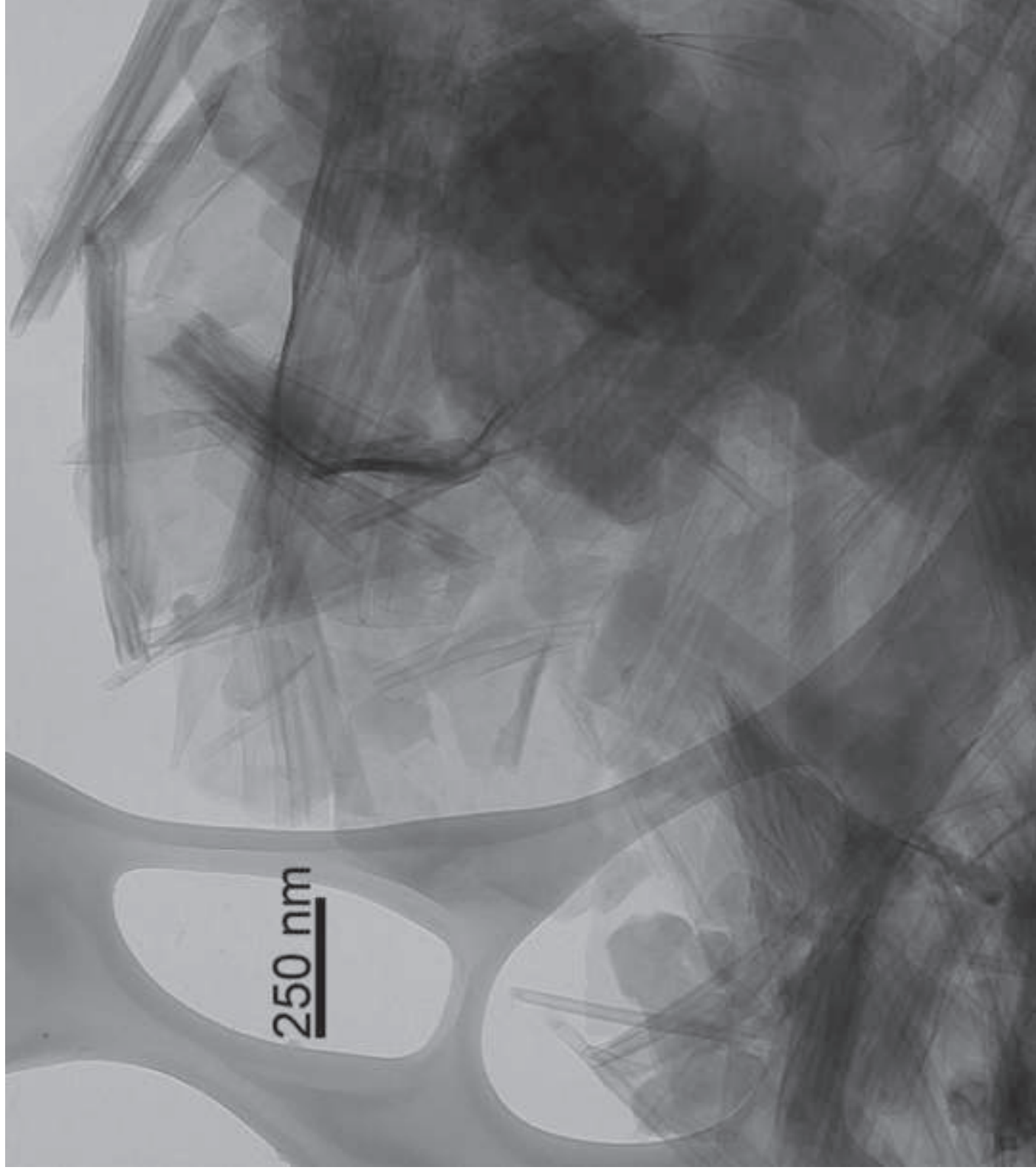


Figure 5

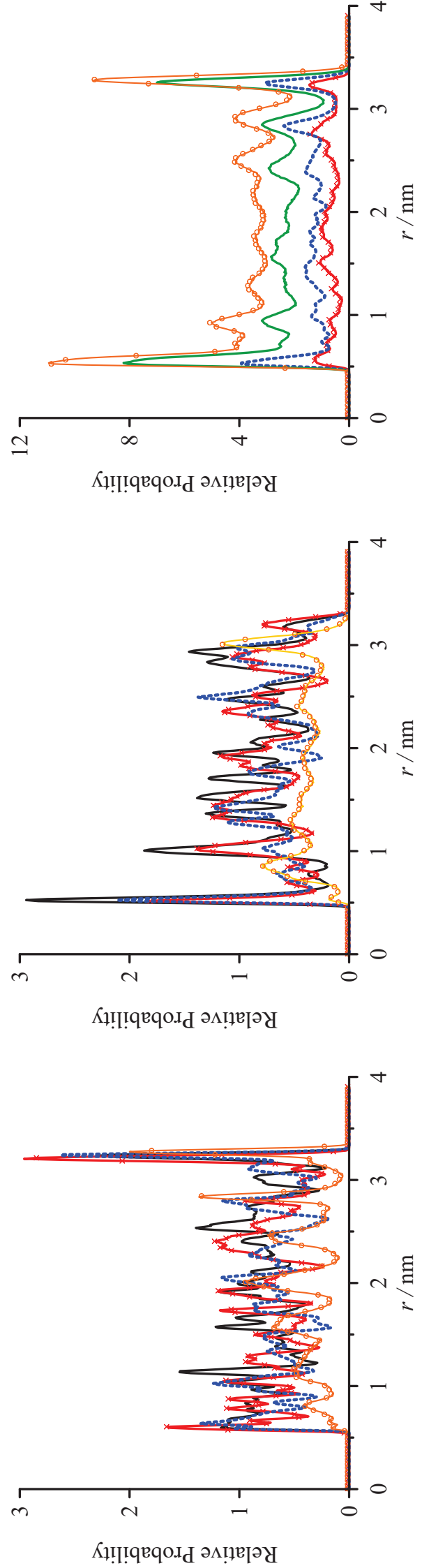


Figure 6

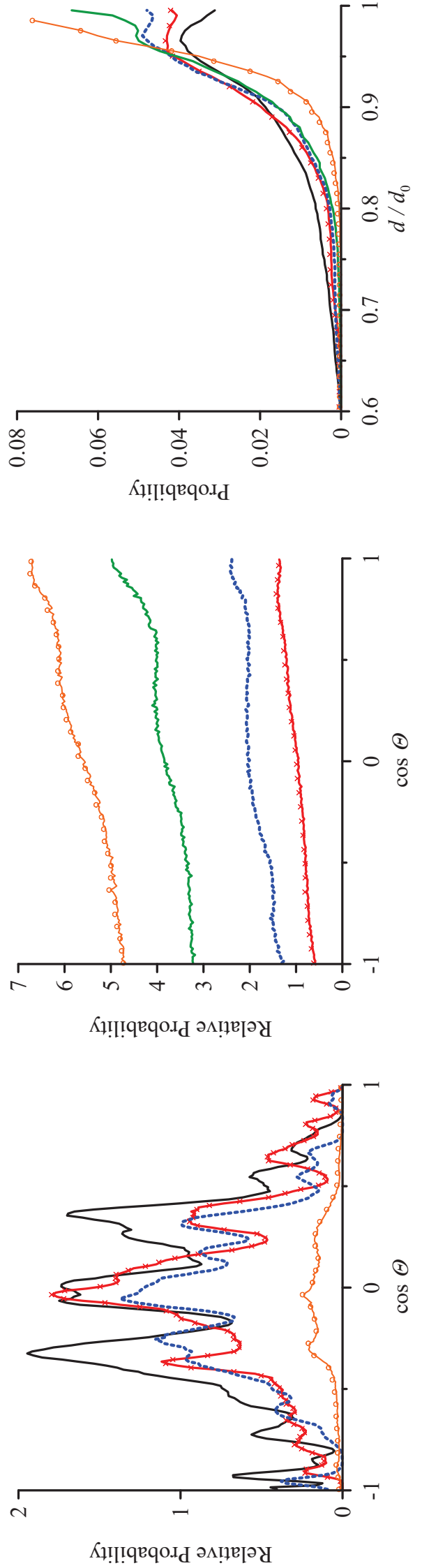


Figure7A
[Click here to download high resolution image](#)

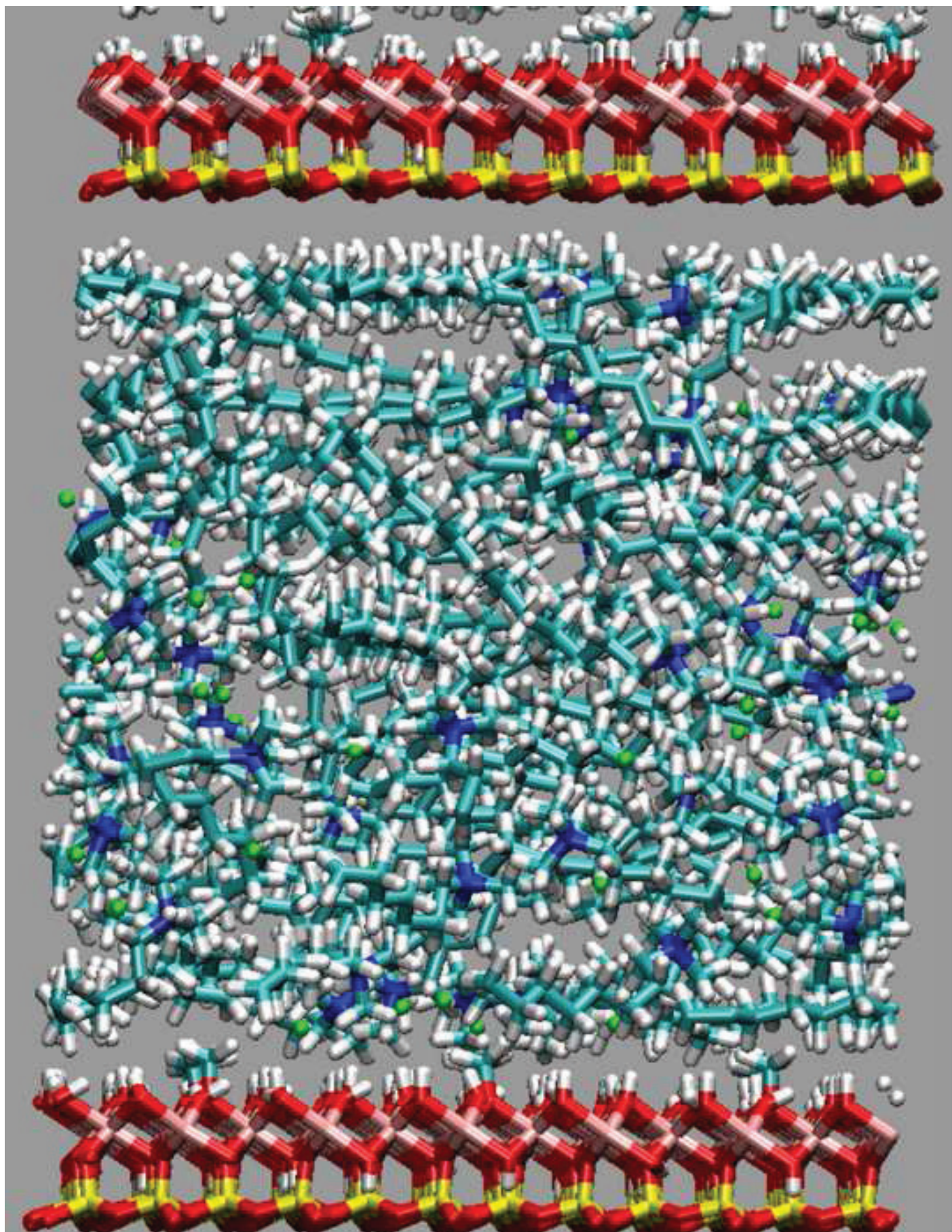


Figure7B
[Click here to download high resolution image](#)

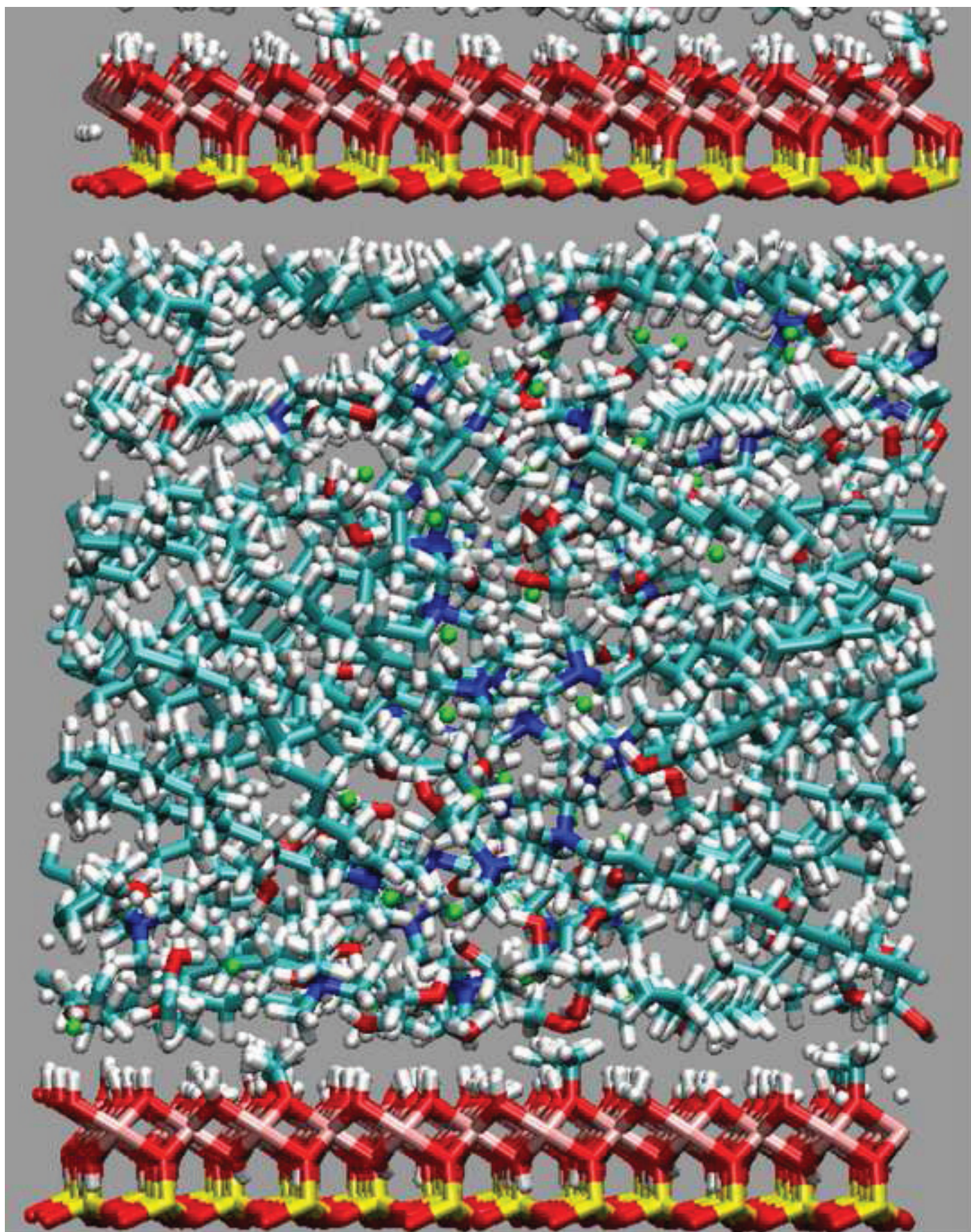


Figure7C
[Click here to download high resolution image](#)

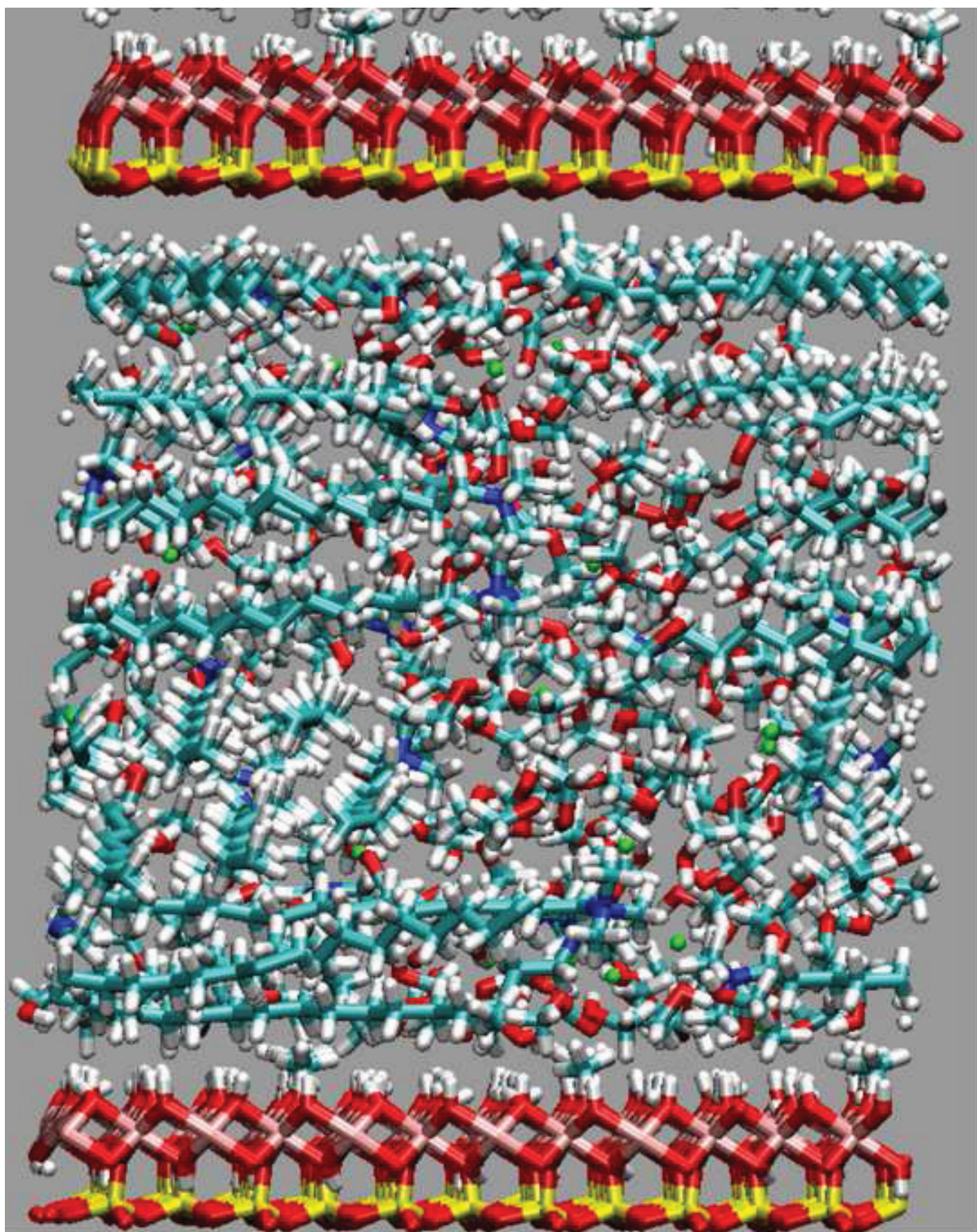


Figure 8) ● 0:1 ◆ 1:1 ▲ 2:1 ◊ 5:1 ○ 10:1

